Geophysical Research Letters

Key Points:
- A model is proposed to explain the time evolution of effusion rate in basaltic eruptions
- It is assumed that the eruption is due to the inflow of a magma pulse in the magma chamber
- A variety of effusion rate functions is possible, depending on the pulse duration and on rheological and geometrical parameters

Correspondence to:
M. Dragoni,
michele.dragoni@unibo.it

A Model for the Effusion Rate Produced by a Magma Pulse

Michele Dragoni[1] [ID] **and Antonello Piombo[1]** [ID]

[1]Dipartimento di Fisica e Astronomia, Alma Mater Studiorum – Università di Bologna, Bologna, Italy

Abstract We assume that a magma pulse enters a magma chamber from the plumbing system, producing an overpressure triggering an effusive volcanic eruption. The chamber is modeled as a spherical cavity in an elastic half-space, connected to the Earth's surface by a vertical conduit, and the magma as an incompressible Newtonian liquid. Overpressure in the chamber is calculated as a function of time during the eruption and has different behaviors depending on the characteristics of the magma pulse and of the volcanic system. The time history of effusion rate is controlled by the pulse duration and the geometrical and rheological parameters of the model. The calculated effusion rates are compared with different classes of effusion rates extrapolated from historical data of Mount Etna, which are asymmetric functions of time. For appropriate values of the model parameters, the calculated time histories are found to fit well those derived from observation.

1. Introduction

Observations show that the effusion rate of magma has a typical dependence on time in basaltic eruptions. In most cases, the effusion rate starts from a small value, increases to a maximum, and later decreases slowly, vanishing at the end of the eruption (e.g., Del Negro et al., 2012; Vicari et al., 2011). Short-term oscillations superposed to the general trend are also observed (Lautze et al., 2004), and a possible explanation was considered in Dragoni and Tallarico (2019).

Effusion rates are often inferred by measurements of radiance of the outpouring lava (Dragoni & Tallarico, 2009; Harris et al., 1997; Harris & Baloga, 2009). Vicari et al. (2011) employed infrared satellite data to estimate lava eruption rates at Mount Etna. They considered flow duration and volume data of about 130 episodes and defined six eruptive classes representing the lava volume in relation to the eruption duration. Volume flow rates ranging from 10 to 140 m^3/s and eruption durations up to 90 days were considered.

In modeling magma effusion, it is generally assumed that the opening of the volcanic conduit is produced by an overpressure in the magma chamber (e.g., Blake, 1981; Gonnermann & Manga, 2012; McLeod & Tait, 1999; Roper & Lister, 2005; Santini et al., 2011). Then pressure decreases as a consequence of magma outflow. The decrease in effusion rate with time can be explained by a simple model (Wadge, 1981), considering that pressure in the magma chamber decreases as the chamber empties. Being proportional to the pressure gradient, the effusion rate decreases until it vanishes.

However, a generally accepted explanation for the initial increase in effusion rate is still lacking. Piombo et al. (2016) showed that mechanical erosion of the conduit wall by the flowing magma may widen the conduit and produce an initial increase in flow rate. In that work, it was assumed that magma inflow in the magma chamber was a slowly increasing function of time, so that any further magma inflow during the eruption was neglected.

This assumption was also made by other authors (e.g., Anderson & Poland, 2016; Segall, 2010). In these models, there is a continuous magmatic connection between the chamber and mantle source. Pressure in the chamber increases gradually with time (in general, a constant rate is assumed) until it reaches a critical value and the eruption takes place. Due to the very small inflow rate, the feeding system has no effect on effusion rate during eruption.

In the present paper, we assume instead that the eruption is due to a magma pulse of finite duration entering the magma chamber from the plumbing system. The aim is to highlight how the finite duration of the magma inflow in the chamber may affect the time history of effusion rate.

The occurrence of magma pulses has been inferred for the feeding of magma chambers prior to eruptions as well as for very long episodes of magma intrusion in the Earth's crust (e.g., Crisp, 1984; Scandone et al., 2007). Paterson et al. (2011) showed that the size of magma pulses moving through volcanic plumbing systems may vary from small dike-like to large diapir-like pulses.

A time-varying injection rate and its effects on mass extraction have been considered by other authors. Karlstrom et al. (2010) modeled stochastic dike flux that provides pulsed input to a magma chamber in a viscoelastic half-space and mapped out parameter regimes of chamber mechanical response. Degruyter and Huber (2014) proposed a model focused on the evolution of the thermodynamic state of the chamber as new magma is injected and showed how the frequency of eruptions depends on the timescale of injection.

2. The Model

We consider a magma chamber placed at some depth in the Earth's crust. The crust is assumed to be a homogeneous and isotropic, elastic half-space with density ρ_1 and Lamé constants λ and μ. The chamber is represented as a cavity filled with an incompressible liquid having density ρ_2.

The model is of course a simplification of a real magma chamber. Assuming an elastic rheology for host rocks is correct only when the timescale of recharge is small compared to processes such as viscous creep of wall rocks (e.g., Dragoni & Magnanensi, 1989; Segall, 2016) and poroelastic pressure diffusion (Liao et al., 2018; Mittal & Richards, 2019).

We also neglect the possibility that the chamber boundary is defined by a rheological transition. In this case, the boundary itself can evolve in time, as yield stress in the mush is overcome. Karlstrom et al. (2012) have shown that there is nonuniqueness in resolving pressure versus volume in these systems and, without other observational constraints, one cannot uniquely assign changes in eruptive flux to pressure changes in the chamber.

The assumption of magma incompressibility may be a limit for shallow chambers, due to volatile exsolution and the presence of gas bubbles. Some works have shown that bubbles can affect the evolution of chamber pressure and eruption rate (Woods & Huppert, 2003) and chamber elastic storativity (Rivalta & Segall, 2008). Bubbles would buffer pressure changes arising from influx variations. However, influx will gradually decrease bubble fraction due to increasing pressure and promote pressurization.

As noticed in section 1, a variety of observations from plutonic and active systems suggests the prevalence of discrete pulses feeding reservoirs. In the absence of data about possible pulse shapes, we choose a simple bell-shaped function of time. We suppose that a magma pulse enters the chamber through the feeding system with a mass flow rate

$$\dot{m}_1(t) = \frac{M}{\sqrt{\pi}T}\, e^{-(t-t_1)^2/T^2}, \tag{1}$$

where the dot indicates derivative with respect to time t, M is the total mass entering the chamber, t_1 is the time corresponding to the maximum of the pulse, and T is a measure of the pulse duration (Figure 1). The cumulative mass entering the chamber is then

$$m_1(t) = \frac{M}{2}\left(1 + \mathrm{erf}\frac{t-t_1}{T}\right). \tag{2}$$

As a consequence of magma inflow, the chamber and the surrounding medium are deformed elastically. We assume that the magma inflow is slow, so that deformation is quasi-static and is solution of the Cauchy-Navier equation

$$(\lambda + \mu)\nabla(\nabla \cdot \mathbf{u}) + \mu\nabla^2\mathbf{u} = 0, \tag{3}$$

where $\mathbf{u}$ is the displacement of the elastic medium. Due to the linearity of the equation, the inflow of a mass m_1 of magma in the chamber produces an overpressure

$$p(t) = k_1 m_1(t), \tag{4}$$

where k_1 is a constant depending on the elastic properties of the medium and on the size of the magma chamber.
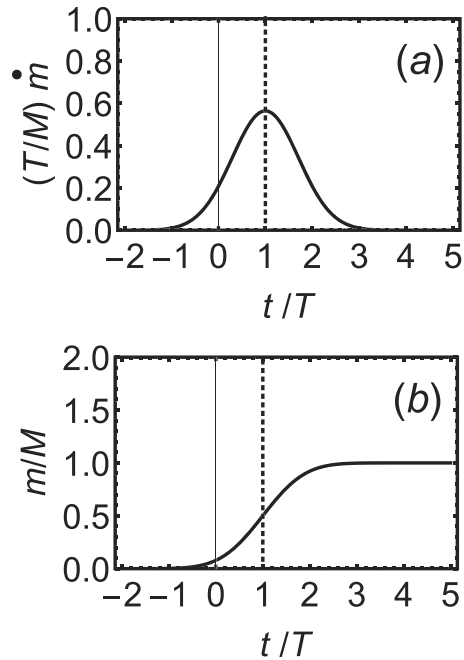
Figure 1. (a) Flow rate of the magma pulse and (b) cumulative flow entering the magma chamber. The onset of eruption is set at $t = 0$, while the magma inflow starts at $t < 0$. The vertical dashed line indicates time t_1, corresponding to the maximum of the pulse ($t_1/T = 1$ has been chosen).

We suppose that at $t = 0$, the overpressure p reaches a critical value p_0 and a vertical tensile fracture, connecting the top of the magma chamber with the Earth's surface, is produced. Then, from (2) and (4), t_1 is given by

$$\text{erfc}\,\frac{t_1}{T} = \frac{2p_0}{k_1 M}. \tag{5}$$

It follows from (5) that, for a given value of p_0, the eruption takes place only if the total mass inflow is greater that a value

$$M_0 = \frac{p_0}{k_1}. \tag{6}$$

On the other hand, for a given mass M, the eruption takes place only if p_0 does not exceed the value $k_1 M$.

The magma outflow rate $\dot{m}_2$ through the volcanic conduit is proportional to the overpressure p, and we set

$$\dot{m}_2(t) = k_2 p(t), \tag{7}$$

where k_2 is a constant depending on the conduit geometry and on the rheology of magma. Considering k_2 a constant implies that the conduit cross section is constant with time. In principle, the section area should depend on the horizontal stress that caused the initial fracture; hence, it should vary with the overpressure p, with effects on flow rate. However, assuming a critical pressure p_0 means that this pressure induces at the top of the chamber a horizontal stress that fractures the medium. This stress decreases very rapidly with distance from the chamber (as the inverse cube of distance), becoming negligible along a volcanic conduit that is kilometers long. Therefore, its influence on the opening or closing of the fracture can be neglected.

During the eruption ($t > 0$), the mass of magma in the chamber changes according to the equation

$$\frac{dm}{dt} = \dot{m}_1 - \dot{m}_2, \tag{8}$$

and the pressure change with time can be written as

$$\frac{dp}{dt} = k_1(\dot{m}_1 - \dot{m}_2). \tag{9}$$

Using (1) and (7) and setting

$$\hat{p}_0 = \frac{k_1 M}{2} \tag{10}$$

and

$$\tau = \frac{1}{k_1 k_2}, \tag{11}$$

we obtain

$$\frac{dp}{dt} + \frac{p}{\tau} = \frac{2\hat{p}_0}{\sqrt{\pi}T} \, e^{-(t-t_1)^2/T^2}, \tag{12}$$

which is a linear, nonhomogeneous differential equation for p with constant coefficients.

3. Overpressure

With the initial condition $p(0) = p_0$, the solution of (12) is

$$p(t) = \hat{p}_0 f(t), \tag{13}$$

where

$$f(t) = \left\{ \operatorname{erfc} \frac{t_1}{T} + e^{\frac{T^2}{4\tau^2} + \frac{t_1}{\tau}} \left[\operatorname{erf}\left(\frac{T}{2\tau} + \frac{t_1}{T} \right) - \operatorname{erf}\left(\frac{T}{2\tau} - \frac{t-t_1}{T} \right) \right] \right\} e^{-\frac{t}{\tau}}. \tag{14}$$

It appears that τ is the characteristic time for the decay of pressure in the magma chamber and for the waning of magma outflow. For very large values of the pulse duration T, (13) reduces to the Wadge (1981) solution

$$p(t) = p_0 e^{-t/\tau}. \tag{15}$$

Figure 2 shows some nondimensional graphs of overpressure during the eruption, where the ratio $p/\hat{p}_0$ is plotted as a function of time, for different values of the ratio t_1/T. The graphs correspond to the same mass M, but to different critical values p_0. Very different behaviors can be observed.

In particular, the maximum $\hat{p}$ of $p(t)$ is reached at a time t_2 that is a discontinuous function of t_1. The discontinuity occurs at $t_1 = t_0$, which is solution of the equation

$$e^{-\frac{t_0}{\tau}} \operatorname{erfc} \frac{t_0}{T} + e^{\frac{T^2}{4\tau^2}} \left[\operatorname{erf}\left(\frac{T}{2\tau} + \frac{t_0}{T} \right) - \operatorname{erf} \frac{T}{2\tau} \right] = \frac{2\tau}{\sqrt{\pi}T}. \tag{16}$$

For $t_1 < t_0$, it results $t_2 = 0$; that is, the maximum overpressure is reached at the onset of the eruption, as in Figure 2a. For $t_1 > t_0$ the instant t_2 is given by the equation

$$f(t_2) - \frac{2\tau}{\sqrt{\pi}T} \, e^{-\frac{(t_2-t_1)^2}{T^2}} = 0. \tag{17}$$

In this case, t_2 is greater than t_1; that is, the maximum overpressure is reached later than the maximum of the magma pulse (Figures 2b and 2c). Both (16) and (17) must be solved numerically. The maximum overpressure $\hat{p}$ as a function of t_1 can be easily calculated from (5) and (12):

$$\hat{p}(t_1) = \begin{cases} \hat{p}_0 \operatorname{erfc} \frac{t_1}{T}, & t_1 < t_0 \\ \frac{2\hat{p}_0 \tau}{\sqrt{\pi}T} \, e^{-\frac{(t_2-t_1)^2}{T^2}}, & t_1 > t_0 \end{cases} . \tag{18}$$

The maximum overpressure is a decreasing function of t_1 with a discontinuity at $t = t_0$ and approaches a constant value when $t_1 \rightarrow \infty$.
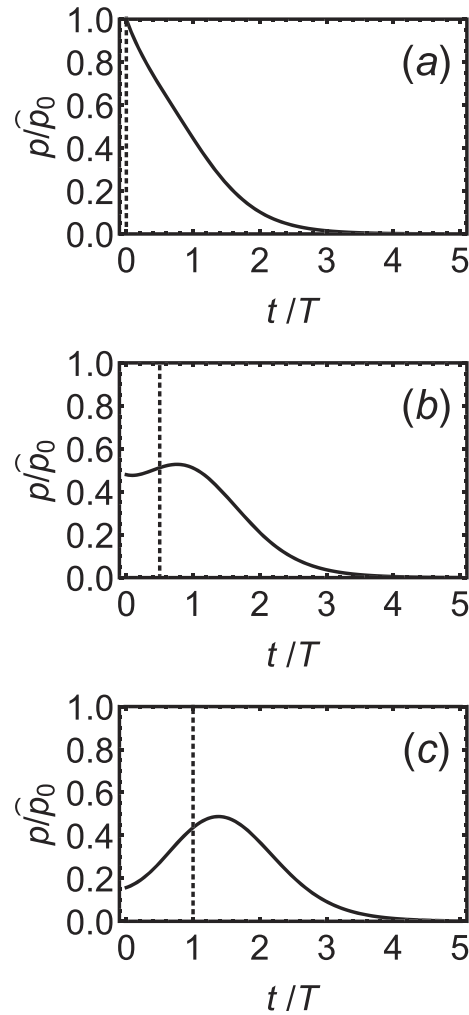
Figure 2. Overpressure p in the magma chamber as a function of time during the eruption, for $\tau/T = 0.5$ and different values of t_1, indicated by the vertical dashed line: (a) $t_1/T = 0$; (b) $t_1/T = 0.5$; and (c) $t_1/T = 1$.

4. Effusion Rate

The mass effusion rate $\dot{m}_2(t)$ from the volcanic vent is given by (7) with $p(t)$ given by (13), the maximum effusion rate occurring when the overpressure is maximum. The cumulative erupted mass is

$$m_2(t) = k_2 \int_0^t p(t')\, dt'. \tag{19}$$

Calculation of the integral yields

$$m_2(t) = \frac{M}{2} \left[\operatorname{erfc} \frac{t_1 - t}{T} - f(t) \right], \tag{20}$$

where M is the total erupted mass. From (7) the volume effusion rate of magma is

$$q(t) = \frac{k_2}{\rho_2} p(t). \tag{21}$$

If we call $\hat{q}_0$ the effusion rate corresponding to the overpressure $\hat{p}_0$, then

$$\frac{q}{\hat{q}_0} = \frac{p}{\hat{p}_0}. \tag{22}$$

Hence, nondimensional graphs of effusion rate coincide with those of overpressure shown in Figure 2. The total erupted volume is

$$V = \frac{M}{\rho_2}. \tag{23}$$

Then, from (21), (13), (10), (11), and (23), the volume effusion rate is

$$q(t) = \frac{V}{2\tau} f(t). \tag{24}$$

5. Assumptions on Geometry and Rheology

In order to obtain dimensional numbers, we must give values to the constants k_1 and k_2. As anticipated, they depend on the geometry of the magma chamber and of the conduit and on the rheological properties of magma. For the sake of simplicity, we assume that the magma chamber is a spherical cavity with radius R. We further assume that the depth of the chamber is at least twice its radius: In this case, the effect of the free surface of the half-space is negligible (Davis, 1986), and we may assume spherical symmetry, so that (3) reduces to

$$\nabla(\nabla \cdot \mathbf{u}) = 0 \tag{25}$$

and the displacement of the cavity wall is (e.g. Landau & Lifshitz, 1970)

$$u(t) = \frac{R}{4\mu} p(t), \tag{26}$$

whence

$$k_1 = \frac{\mu}{\pi \rho_1 R^3}. \tag{27}$$

According to (6) and (27), the minimum mass necessary for the eruption is

$$M_0 = \frac{\pi p_0 \rho_1 R^3}{\mu}. \tag{28}$$

We further assume that magma is a homogeneous and isotropic Newtonian liquid with viscosity η and that the conduit connecting the magma chamber to the Earth's surface is a cylinder with length h and an elliptic cross section with semiaxes a and b. An elliptic cross section can represent a wide range of shapes, according to the value of eccentricity, from almost circular vents to very long and narrow fissures. Then, from the expression of flow rate in the conduit (Dragoni & Santini, 2007), we obtain

$$k_2 = \frac{\pi \rho_2}{4\eta h} \frac{a^3 b^3}{a^2 + b^2}. \tag{29}$$

According to (11), the waning time τ is then

$$\tau = \frac{4\eta \rho_1 h R^3 (a^2 + b^2)}{\mu \rho_2 a^3 b^3}. \tag{30}$$

It depends on all the geometrical and rheological parameters of the model. A large value of τ means that magma needs a longer time to outflow, because of a high viscosity and/or a large size and depth of the magma chamber and/or a narrow conduit. In terms of the area A and eccentricity ϵ of the volcanic vent, we can write

$$\tau = \frac{4\pi^2 \eta \rho_1 h R^3 (2 - \epsilon^2)}{\mu \rho_2 A^2 \sqrt{1 - \epsilon^2}}, \tag{31}$$

showing that, for a given area A, τ is almost constant for small values of ϵ and may become large only for volcanic fissures with $\epsilon > 0.9$, due to the decrease of flow rate in the conduit.

Table 1
The Basic Model Parameters

a	Semimajor axis of volcanic conduit
b	Semiminor axis of volcanic conduit
h	Length of volcanic conduit
p_0	Critical overpressure
R	Radius of magma chamber
T	Duration of magma pulse
V	Total erupted volume
η	Viscosity of magma
μ	Rigidity of the crust
ρ_1	Density of the crust
ρ_2	Density of magma

6. Numerical Results

We wish to investigate whether the inflow of a magma pulse into the magma chamber can reproduce the typical effusion rates observed in basaltic eruptions, showing an initial increase followed by a slower decrease. To this aim, we consider the different classes of effusion rates extrapolated from historical data of Mount Etna by Vicari et al. (2011) and Del Negro et al. (2012).

There are 11 basic parameters in the model, which are listed in Table 1. The other parameters can be calculated from these. In order to reproduce the different classes of effusion rates, we assign a fixed value to seven parameters. In particular, we assume that the Earth's crust has a rigidity $\mu = 30$ GPa and a density $\rho_1 = 3,000$ kg/m^3 and that magma has a density $\rho_2 = 2,600$ kg/m^3 and a viscosity $\eta = 10^3$ Pa s. We consider a conduit length $h = 12$ km and a volcanic fissure with semiaxes $a = 20$ m and $b = 1$ m, corresponding to an eccentricity $\epsilon \simeq 0.999$ and to an area $A \simeq 63$ m^2.

For the remaining four parameters V, T, R, and p_0, we choose different sets of values as shown in Table 2. In particular, for a comparison with effusion rates given by Del Negro et al. (2012), we choose values of V equal to 30, 100, and 200×10^6 m^3. For each choice of V, two different values of pulse duration T, magma chamber radius R, and critical overpressure p_0 are considered.

From the assumed values of the 11 parameters, τ is obtained from (30), and t_1 is calculated numerically from (5), where k_1 and M are given by (27) and (23), respectively. Finally, the effusion rate is calculated from (24).

According to (5), t_1 can assume any real value. However, negative values would correspond to very high values of p_0, which are not realistic. If p_0 is in the order of 1 MPa, only a fraction of the total mass M is required to attain p_0, and the value of t_1 is typically in the order of T.

A characteristic feature of the observed effusion rates is that they are asymmetric with respect to time, the waxing phase being shorter than the waning phase. This might be a consequence of the fact that magma pulses are themselves asymmetric. However, the present model shows that the curve $\dot{m}_2(t)$ of outflow rate is not necessarily similar to the curve $\dot{m}_1(t)$ of inflow rate. In particular, the effusion rate can be asymmetric even though the magma pulse is symmetric. It becomes symmetric only in the limit case $T \gg \tau$. The six cases considered below are such that $T < \tau$.

Table 2
The Six Cases Considered in Figure 4

Parameter	a1	a2	b1	b2	c1	c2	Units
V	30	30	100	100	200	200	10^6 m^3
T	4	12	3	10	3	10	d
R	2	3	2	3	2	3	km
p_0	0.8	0.5	0.8	0.5	0.8	0.5	MPa

Note. The other parameters are fixed: $a = 20$ m, $b = 1$ m, $h = 12$ km, $\eta = 10^3$ Pa s, $\mu = 30$ GPa, $\rho_1 = 3,000$ kg/m^3, $\rho_2 = 2,600$ kg/m^3.
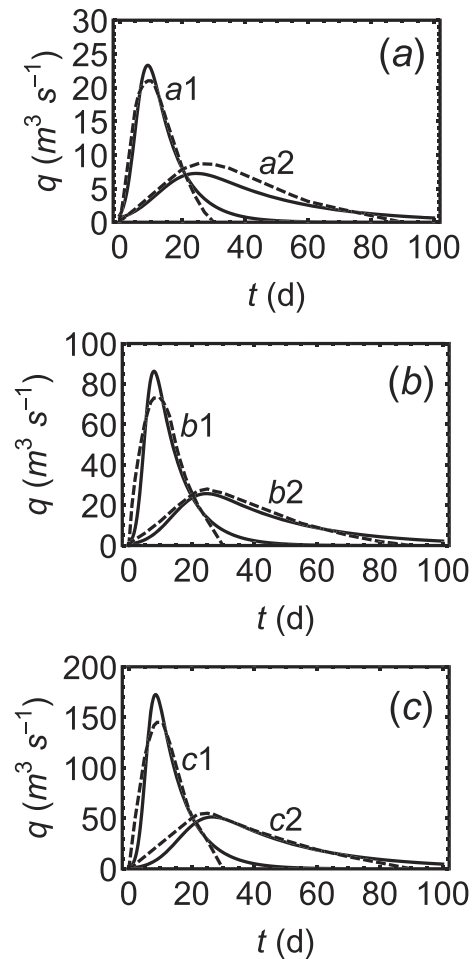
Figure 3. Effusion rate $q(t)$ as a function of time, calculated for the six cases shown in Table 2 (solid lines). The dashed lines are flow rates of the six different classes established for Mount Etna by Vicari et al. (2011) and Del Negro et al. (2012).

According to (31), the waning time τ is proportional to the volume of the magma chamber. Since the same volume is chosen in cases $(a1)$, $(b1)$, and $(c1)$, they share the same value $\tau \simeq 9$ days. Having similar values of T, the three cases have also a similar duration of the eruption, approximately 40 days. Analogously, cases $(a2)$, $(b2)$, and $(c2)$ share the value $\tau \simeq 29$ days, and the duration of the eruption is approximately 100 days.

The curves plotted in Figure 3 fit reasonably well those shown by Del Negro et al. (2012). It results that the observed effusion rates are obtained when a shorter pulse duration is associated with a smaller magma chamber and a higher critical overpressure.

The time history of effusion rate is sensible to relatively small changes in most model parameters. According to (24), q is a function of the magma input V and of the three times T, t_1, and τ. Times T and t_1 appear in the ratio t_1/T, which mainly depends on the magma input, the critical overpressure, and the volume of magma chamber.

The waning time τ is mainly controlled by magma viscosity, volume, and depth of the magma chamber, area, and eccentricity of the eruptive vent. The ratio τ/T has a strong effect on the time evolution of effusion rate. Changes in crustal rigidity μ and in the density ratio ρ_1/ρ_2, which also appear in the expressions for t_1 and τ, have a minor effect due to their limited variation range.

We also check the model for a specific eruption described by Vicari et al. (2011), with effusion rate data obtained from satellite-measured heat flux. It was a small eruption, which started on 12 January 2011 and lasted approximately 36 hr. Considering the variability range of lava parameters, the authors proposed two limit cases, with maximum effusion rates of about 20 and 60 m³/s, respectively. We model the two cases by
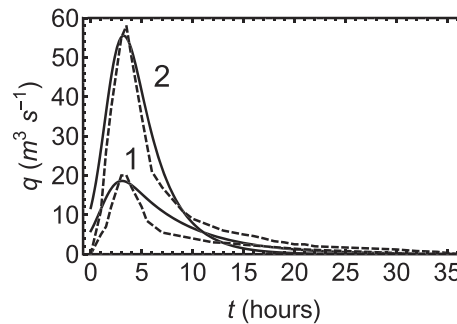
Figure 4. Effusion rate $q(t)$ as a function of time (solid lines), calculated for the two cases considered by Vicari et al. (2011) for the 12 January 2011 eruption on Mount Etna, compared with data (dashed lines).

assuming erupted volumes $V_1 = 0.6 \times 10^6$ and $V_2 = 1.2 \times 10^6$ m³, respectively. The theoretical curves fit reasonably well the observed ones, if one chooses $T = 2$ hr, $p_0 = 0.6$ MPa, $\eta = 200$ Pa s, and $R = 1.2$ km for both cases, with different depths $h_1 = 8$ km and $h_2 = 4$ km, the other parameters being the same as before (Figure 4).

7. Conclusions

We proposed a model simulating the inflow of a magma pulse into a magma chamber, the pressurization of the chamber produced by the mass inflow, and the subsequent outflow through a volcanic conduit. The process is governed by the size and duration of the magma pulse, by the geometrical properties of the chamber and of the conduit, by the elastic properties of the Earth's crust, and by the rheological properties of magma.

We found that the overpressure in the magma chamber during the eruption may have different behaviors, depending on the characteristics of the magma pulse and of the volcanic system: In particular, the maximum overpressure can occur later than the maximum of the pulse. The magma effusion rate has an initial increase and a subsequent decrease that are controlled by the pulse duration and waning time, depending on the geometrical and rheological parameters of the model.

The calculated effusion rates are compared with different classes of effusion rates extrapolated from historical data of Mount Etna, which are asymmetric functions of time with a relatively fast increase and a much slower decrease. The effusion rate for a specific eruption occurred in 2011 has been also reproduced.

For appropriate values of the model parameters, the calculated time histories of effusion rate are found to fit well the observed ones. It is remarkable that curves very similar to the observed ones can be obtained by assigning fixed values to most model parameters and varying only few of them, such as the size and duration of the magma pulse, the size of the magma chamber, and the critical overpressure for eruption.

References

Anderson, K. R., & Poland, M. P. (2016). Bayesian estimation of magma supply, storage, and eruption rates using a multiphysical volcano model: Kilauea Volcano, 2000–2012. *Earth and Planetary Science Letters*, *447*, 161–171.

Blake, S. (1981). Volcanism and the dynamics of open magma chamber. *Nature*, *289*, 783–785.

Crisp, J. A. (1984). Rates of magma emplacement and volcanic output. *Journal of Volcanology and Geothermal Research*, *20*, 177–211. https://doi.org/10.1016/0377-0273(84)90039-8

Davis, P. M. (1986). Surface deformation due to inflation of an arbitrarily oriented triaxial ellipsoidal cavity in an elastic half-space, with reference to Kilauea volcano, Hawaii. *Journal of Geophysical Research*, *91*(B7), 7429–7438.

Degruyter, W., & Huber, C. (2014). A model for eruption frequency of upper crustal silicic magma chambers. *Earth and Planetary Science Letters*, *403*, 117–130.

Del Negro, C., Cappello, A., Neri, M., Bilotta, G., Herault, A., & Ganci, G. (2012). Lava flow hazards at Mount Etna: Constraints imposed by eruptive history and numerical simulations. *Scientific Reports*, *3*, 3493–3493.

Dragoni, M., & Magnanensi, C. (1989). Displacement and stress produced by a pressurized, spherical magma chamber, surrounded by a viscoelastic shell. *Physics of the Earth and Planetary Interiors*, *56*, 316–328.

Dragoni, M., & Santini, S. (2007). Lava flow in tubes with elliptical cross sections. *Journal of Volcanology and Geothermal Research*, *160*, 239–248. https://doi.org/10.1016/j.jvolgeores.2006.09.008

Dragoni, M., & Tallarico, A. (2009). Assumptions in the evaluation of lava effusion rates from heat radiation. *Geophysical Research Letters*, *36*, L08302. https://doi.org/10.1029/2009GL037411

Dragoni, M., & Tallarico, A. (2019). Changes in lava effusion rate from a volcanic fissure due to pressure changes in the conduit. *Geophysical Journal International*, *216*, 692–702.

Gonnermann, H. M., & Manga, M. (2012). Dynamics of magma ascent in the volcanic conduit. In S. A. Fagents & T. K. P. Gregg (Eds.), *Modeling Volcanic Processes: The Physics and Mathematics of Volcanism* (pp. 55–84). Cambridge: Cambridge University Press.

Harris, A. J. L., & Baloga, S. M. (2009). Lava discharge rates from satellite-measured heat flux. *Geophysical Research Letters*, *36*, L19302. https://doi.org/10.1029/2009GL039717

Harris, A. J. L., Blake, S., Rothery, D. A., & Stevens, N. F. (1997). A chronology of the 1991 to 1993 Mount Etna eruption using advanced very high resolution radiometer data: Implications for real-time thermal volcano monitoring. *Journal of Geophysical Research*, *102*, 7985—8003.

Karlstrom, L., Dufek, J., & Manga, M. (2010). Magma chamber stability in arc and continental crust. *Journal of Volcanology and Geothermal Research*, *190*, 249–270.

Karlstrom, L., Rudolph, M. L., & Manga, M. (2012). Caldera size modulated by the yield stress within a crystal-rich magma reservoir. *Nature Geoscience*, *5*, 402–405.

Landau, L. D., & Lifshitz, E. M. (1970). *Theory of elasticity* (2nd ed.), (pp. 165). Oxford: Pergamon Press.

Lautze, N. C., Harris, A., Bailey, J. E., Ripepe, M., Calvari, S., Dehn, J., et al. (2004). Pulsed lava effusion at Mount Etna during 2001. *Journal of Volcanology and Geothermal Research*, *137*(1-3), 231–246.

Liao, Y., Soule, S. A., & Jones, M. (2018). On the mechanical effects of poroelastic crystal mush in classical magma chamber models. *Journal of Geophysical Research: Solid Earth*, *123*, 9376–9406. https://doi.org/10.1029/2018JB015985

McLeod, P., & Tait, S. (1999). The growth of dykes from magma chambers. *Journal of Volcanology and Geothermal Research*, *92*, 231–245.

Mittal, T., & Richards, M. A. (2019). Volatile degassing from magma chambers as a control on volcanic eruptions. *Journal of Geophysical Research: Solid Earth*, *124*, 7869–7901. https://doi.org/10.1029/2018jb016983

Paterson, S. R., Okaya, D., Memeti, V., Economos, R., & Miller, R. B. (2011). Magma addition and flux calculations of incrementally constructed magma chambers in continental margin arcs: Combined field, geochronologic and thermal modeling studies. *Geosphere*, *7*, 1439—1468. https://doi.org/10.1130/GES00696.1

Piombo, A., Tallarico, A., & Dragoni, M. (2016). Role of mechanical erosion in controlling the effusion rate of basaltic eruptions. *Geophysical Research Letters*, *43*, 8970–8977. https://doi.org/10.1002/2016GL069737

Rivalta, E., & Segall, P. (2008). Magma compressibility and the missing source for some dike intrusions. *Geophysical Research Letters*, *35*, L04306. https://doi.org/10.129/2007GL032521

Roper, S. M., & Lister, J. R. (2005). Buoyancy-driven crack propagation from an over-pressured source. *Journal of Fluid Mechanics*, *536*, 79–98.

Santini, S., Tallarico, A., & Dragoni, M. (2011). Magma ascent and effusion from a tensile fracture propagating to the Earth's surface. *Geophysical Journal International*, *186*, 681–698. https://doi.org/10.1111/j.1365-246X.2011.05060.x

Scandone, R., Cashman, K. V., & Malone, S. D. (2007). Magma supply, magma ascent and the style of volcanic eruptions. *Earth and Planetary Science Letters*, *253*, 513–529. https://doi.org/10.1016/j.epsl.2006.11.016

Segall, P. (2010). *Earthquake and volcano deformation*. Princeton NJ: Princeton University Press.

Segall, P. (2016). Repressurization following eruption from a magma chamber with a viscoelastic aureole. *Journal of Geophysical Research*, *121*, 8501–8522. https://doi.org/10.1002/2016JB013597

Vicari, A., Ganci, G., Behncke, B., Cappello, A., Neri, M., & Negro, C. D. e. l. (2011). Near-real-time forecasting of lava flow hazards during the 12–13 January 2011 Etna eruption. *Geophysical Research Letters*, *38*, L13317. https://doi.org/10.1029/2011GL047545

Wadge, G. (1981). The variation of magma discharge during basaltic eruptions. *Journal of Volcanology and Geothermal Research*, *11*, 139–168.

Woods, A. W., & Huppert, H. E. (2003). On magma chamber evolution during slow effusive eruptions. *Journal of Geophysical Research*, *B8*(2403), 108. https://doi.org/10.1029/2002JB002019